World Academy of Science, Engineering and Technology
International Journal of Geological and Environmental Engineering
Vol:16, No:10, 2022

Identification of Igneous Intrusions in South Zallah Trough, Sirt Basin, Libya

Mohamed A. Saleem

Open Science Index, Geological and Environmental Engineering Vol:16, No:10, 2022 publications.waset.org/10012720.pdf

***Abstract*—**Using mostly seismic data, this study intends to show some examples of igneous intrusions found in some areas of the Sirt Basin and explore the period of their emplacement as well as the interrelationships between these sills. The study area is located in the south of the Zallah Trough, south-west Sirt basin, Libya. It is precisely between the longitudes 18.35° E and 19.35° E, and the latitudes 27.8° N and 28.0° N. Based on a variety of criteria that are usually used as marks on the igneous intrusions, 12 igneous intrusions (Sills), have been detected and analysed using 3D seismic data. One or more of the following were used as identification criteria: the high amplitude reflectors paired with abrupt reflector terminations, vertical offsets, or what is described as a dike-like connection, the violation, the saucer form, and the roughness. Because of their laying between the hosting layers, the majority of these intrusions are classified as sills. Another distinguishing feature is the intersection geometry link between some of these sills. Every single sill has given a name just to distinguish the sills from each other such as S-1, S-2, and … S-12. To avoid the repetition of description, the common characteristics and some statistics of these sills are shown in summary tables, while the specific characters that are not common and have been noticed for each sill are shown individually. The sills, S-1, S-2, and S-3, are approximately parallel to one other, with the shape of these sills being governed by the syncline structure of their host layers. The faults that dominated the strata (pre-upper Cretaceous strata) have a significant impact on the sills; they caused their discontinuity, while the upper layers have a shape of anticlines. S-1 and S-10 are the group's deepest and highest sills, respectively, with S-1 seated near the basement's top and S-10 extending into the sequence of the upper cretaceous. The dramatic escalation of sill S-4 can be seen in North-South profiles. The majority of the interpreted sills are influenced and impacted by a large number of normal faults that strike in various directions and propagate vertically from the surface to the basement's top. This indicates that the sediment sequences were existed before the sill's intrusion, deposited, and that the younger faults occurred more recently. The pre-upper cretaceous unit is the current geological depth for the Sills S-1, S-2 … S-9, while Sills S-10, S-11, and S-12 are hosted by the Cretaceous unit. Over the sills S-1, S-2, and S-3, which are the deepest sills, the pre-upper cretaceous surface has a slightly forced folding, these forced folding is also noticed above the right and left tips of sill S-8 and S-6, respectively, while the absence of these marks on the above sequences of layers supports the idea that the aforementioned sills were emplaced during the early upper cretaceous period.

***Keywords*—**Sirt Basin, Zallah Trough, igneous intrusions, seismic data.

I. Introduction

The study area is located in the south of the Zallah Trough, south-west Sirt basin, Libya (see Fig. 1). It is precisely between the longitudes 18.35° E and 19.35° E, and the latitudes 27.8° N and 28.0° N.

The new geophysical investigation using the knowledge of the plate boundary concepts makes a better understanding of the relationship between the tectonics and the magmatism activity [1]. The relationship between the emplacements of the igneous rocks and the tectonics events by which those rocks have been produced is now excessively accepted [2]-[4]. This paper aims to present some examples of the igneous intrusions distributed in a part of the Sirt Basin and investigates the time of their emplacement, and the interrelations between these sills, using mainly the seismic data.

II. History of Magmatism in Libya

Al Awaynat inlier in the far south-west is the oldest igneous rock in Libya, a number of studies about this inlier have been conducted by [5]-[7]. The radiometric age dating reveals that these rocks have been formed between 2900 Ma to 2500 Ma, and the main component of them is the Granulites and gneisses, [8] documented that the Al Awaynat rock rounded by a ring of younger Cenozoic intrusion.

The isotopic age dating applied to hundreds of basement rock samples collected from different wells reveals that these basement igneous rocks have ages range between 670 Ma and 460 Ma [7]. The isotopic age dating for the upper part of the Tibesti massif on the western side shows that the ages of these rocks range from 526 Ma to 790 Ma [9].

Some previous studies confirmed the presence of Precambrian age rocks in the Cyrenaica Platform [10], while the basalt eruption in the offshore related to the mid to late Permian.

The potassium-argon (K-Ar) method proved that the penetrated granite in the Waddan Horst has an age of 256 Ma and the micro-syenite sills distributed in the Amal area have an age of 245 Ma [4]. The associated magmatism of the rifting that caused the break-up of Pangaea presented in Libya by the emplacement of the granodiorite in the Waddan Platform at 230 Ma and the Granodiorite in the Amal Filed at 207 Ma, these events occurring in the same period of the initial rifting of the Mediterranean region [11]. The volcanic activity associated with the Tibesti-Sirt Arch rifting continues up to the early Cretaceous. According to [12], the Sirt Arch, was at that time existing over a 'fixed-mantle hot-spot' that made the rocks of the crust above them got thinning and weakening.

Mohamed A. Saleem is with Libyan Petroleum Institute, Libya (e-mail: m.saleem@lpilibya.com).

Open Science Index, Geological and Environmental Engineering Vol:16, No:10, 2022 publications.waset.org/10012720.pdf

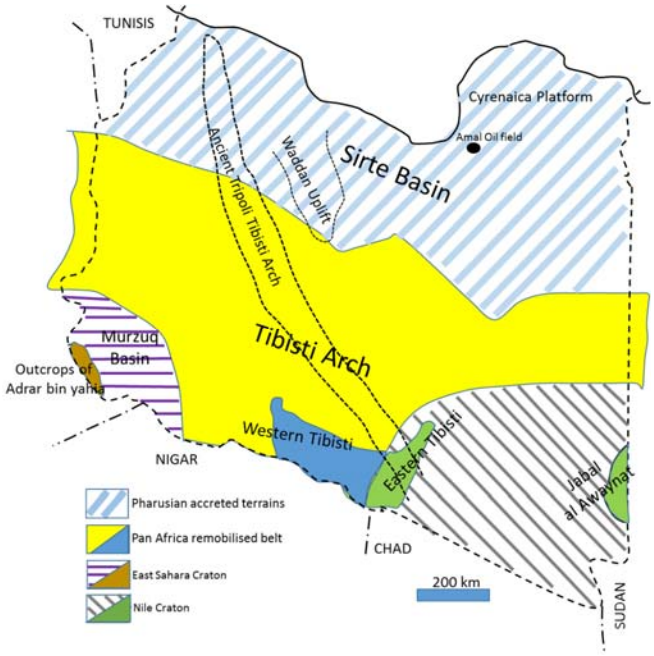

Fig. 1 Map of Libya showing the location of the study area and the places of magma activity (see the text), modified from [13]

At the Pelagian Shelf, the magmatism increased due to the late Cretaceous strike-slip faulting (sinistral) and the prolonged rifting that dominated the area at that time [4].

In the Ajdabiyah Trough and Cyrenaica platform, the intensive basaltic lava eruption occurred along the ancient Tripoli-Tibesti Uplift' since Tortonian time [13]. The eruption of the volcanic rocks in the area extending from Gharyans to the Tibesti Massif persisted from Eocene to the recent time [14]. In the Al Harouge al Aswad area, the magmatism has only recently stopped. Table I summarizes the previous magmatism events and ages in sequence.

TABLE I
SUMMARY OF VOLCANIC EVENTS AND RADIOACTIVE AGES OF ROCKS IN LIBYA [14]

Area, event and rocks	Radiometric Age
Al Awaynat inlier (Granulites and gneisses)	2900 Ma-2500 Ma
Rhyolites of western part of upper Tibisti massive	790 Ma-526 Ma
Sirte basin igneous rock	670 Ma-460 Ma
Granite of the Waddan Horst	256 Ma
Off shore Libya	254 Ma
The microsyenite sills in the Amal area	245 Ma
Granodiorite of the Waddan platform	230 Ma
Granodiorite of the Amal oil field	207 Ma
Some granite intrusion in the Sirte Basin	152 Ma-122 Ma
volcanic rocks were erupted in the area from Tibisti Massif to Gharyan along the line of the ancient Tripoli-Tibisti Uplift	Since Eocene to recent time (55.8 Ma-0 Ma)
The huge basaltic and basanic lava were erupted along the line of the ancient Tripoli-Tibisti Uplift	Since Tortonian 11.6 Ma

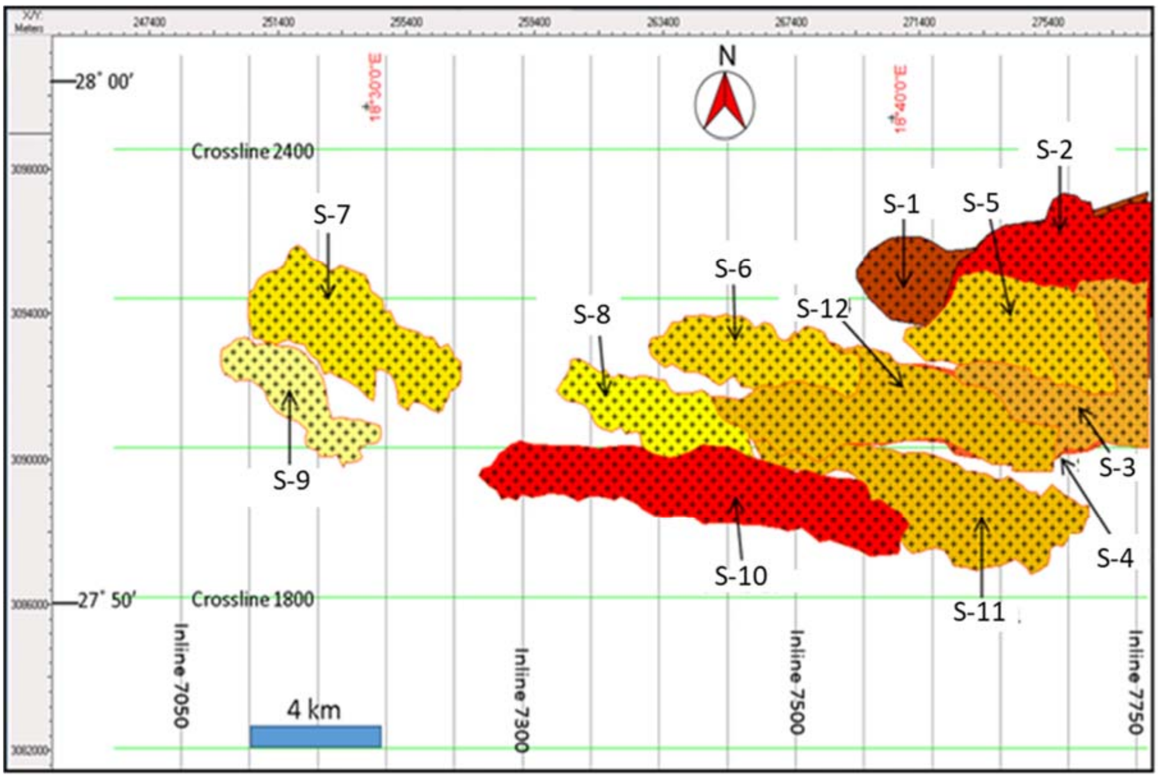

Fig. 2 Map showing the relative distribution of the detected sills in the study area.

III. Interpretation of the Igneous Intrusions

A group of igneous intrusions has been identified and interpreted, based on the number of characteristics that indicate the presence of igneous intrusions in the seismic data. The

Open Science Index, Geological and Environmental Engineering Vol:16, No:10, 2022 publications.waset.org/10012720.pdf

identification criteria could be one or multi of the following: strong reflectors combined with the abrupt termination of these reflectors, the vertical offsets or what known as a dike-like connection. The saucer-shape, the roughness, and the transgression are often common properties for the shallow intrusions [15]. Most of these intrusions are most likely considered as a sills type, due to their concordant with the hosting layers, one more identification character is the intersection geometry relationship between the complexes of the sills.

IV. Sills Identification and Description

12 igneous intrusions (sills) have been identified and interpreted through 3D seismic data, as shown in Figs. 2 and 3. These sills have been assigned different names, starting from S-1 to S-12 to make it easier to distinguish them apart. Tables II and III summarize the common characteristics and several statistics of these interpreted sills. The specific characters that are not common and have been noticed will be stated during describing each sill.

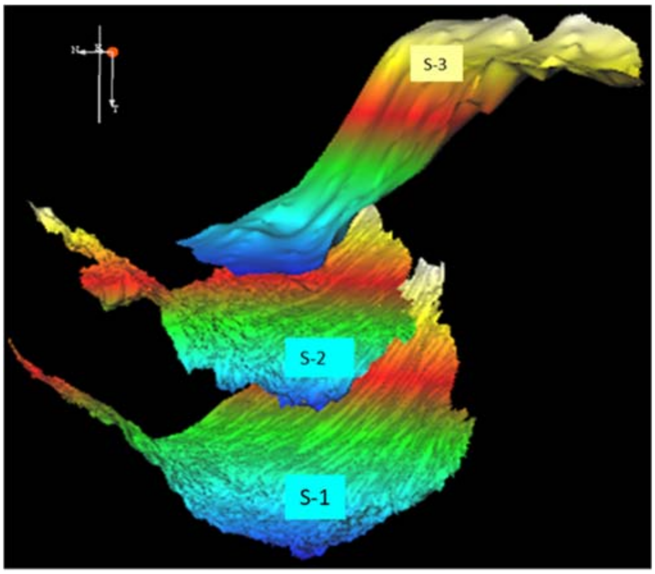

Fig. 3 The relative positions of sills S-1, S-2, and S-3, in oblique view, sill S-2 seems to be nested in sill S-1

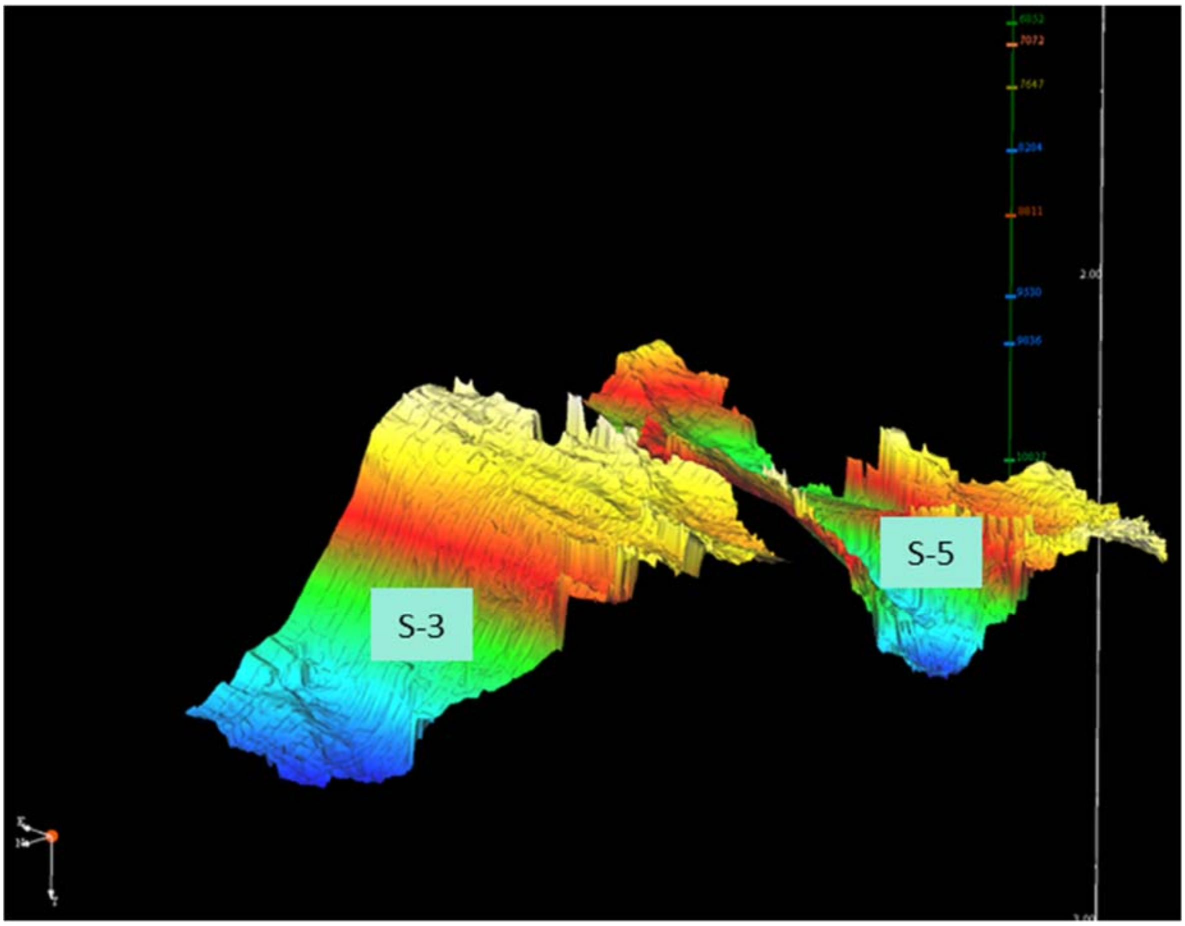

Fig. 4 Relative relationships of Sill S-3 and S-5

In addition to the common characteristics shown in Table III and Table II, the sill S-1 at the western side appears as a sub-horizontal sheet where it nearly connected with the sill S-2. The E-W profiles show the positioning of the sill horizontally and concordantly with the accommodate layer.

The sill was emplaced within the lower Cretaceous deposits. These deposits consist of sandstone as the main formation, interbedded with dolomite and clay, at a depth between 3.8 km

Open Science Index, Geological and Environmental Engineering Vol:16, No:10, 2022 publications.waset.org/10012720.pdf

and 4.6 km.

Sill S-2 characterized generally by a smooth edge disturbed to the north by a small protuberance. It has a saucer shape on the east side; this shape converts to a dipping sheet on the western side. Based on this shape, the proposed depth of emplacement was relatively shallow. The depth at the present-day ranges from 4.2 km to 5 km. In the western part, the amplitude is reduced due to the overlapped of this area by the sill S-3 especially where the two sills become too close.

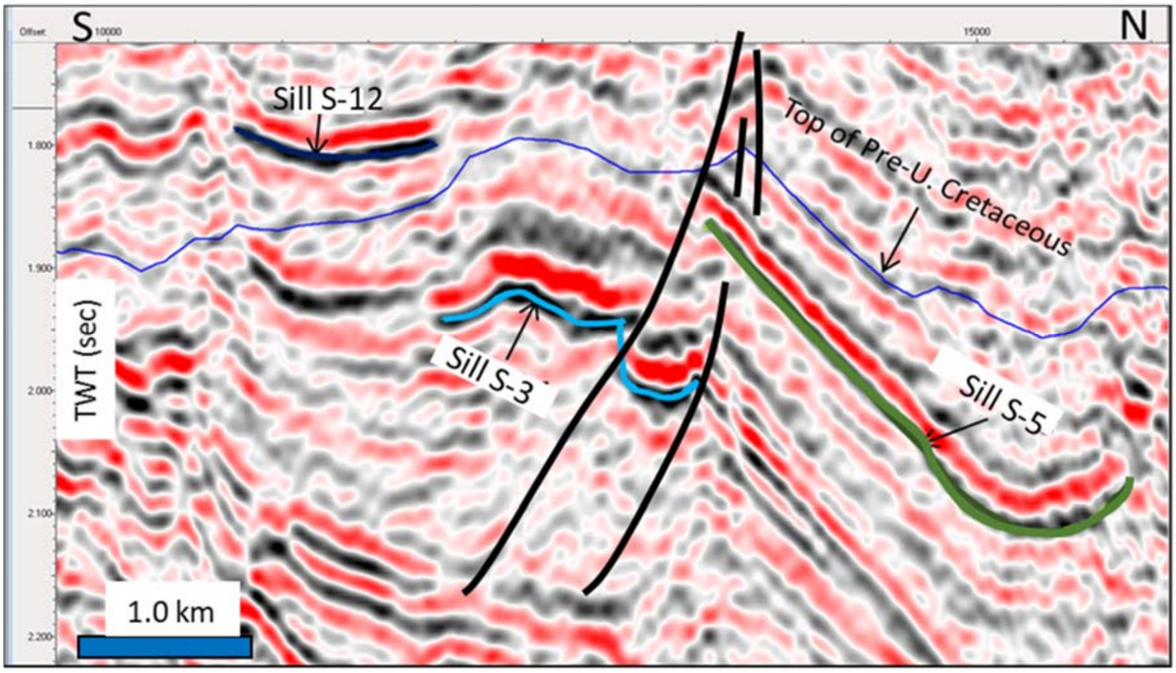

Fig. 5 View of sill-S-3, sill-S-5 and sill-S-12 in seismic profile and their level relative to one of the interpreted horizons

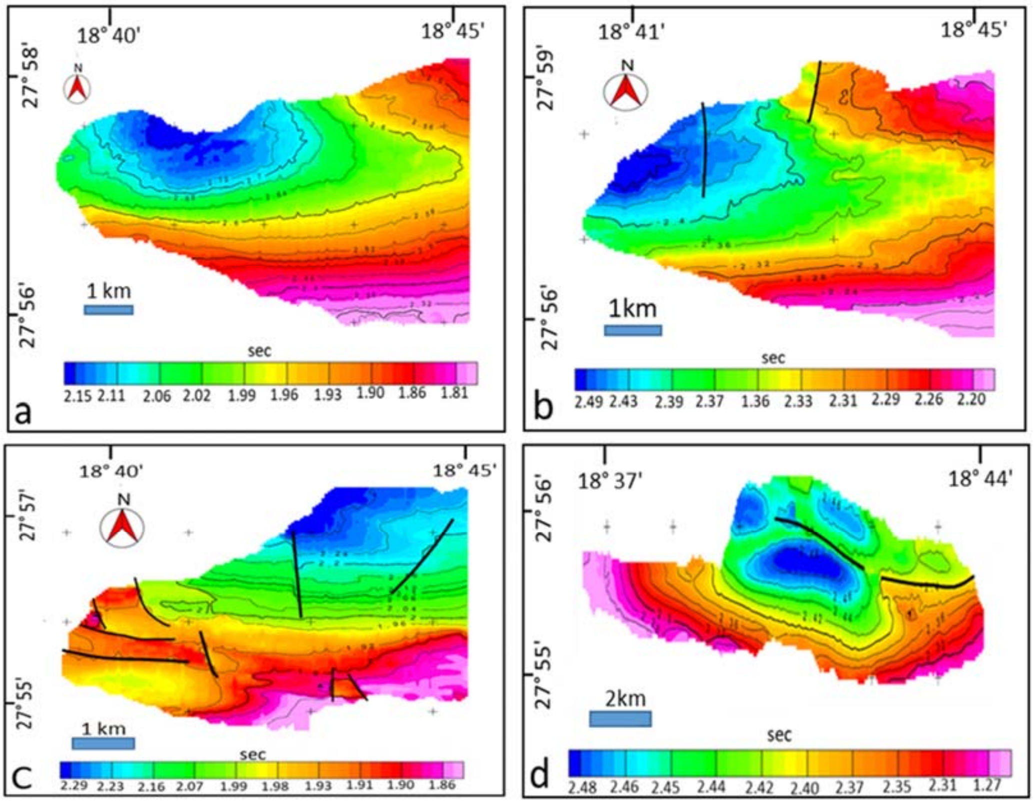

Fig. 6 Plan views of number of sills: (a) sill S-1 (b) sill S-2, (c) sill S-3, and (d) sill S-4

Open Science Index, Geological and Environmental Engineering Vol:16, No:10, 2022 publications.waset.org/10012720.pdf

TABLE II
SOME COMMON CHARACTERISTICS OF THE INTERPRETED SILLS

Sill Name	General shape	Down dipping	Extending	Lower amplitude	Higher amplitude	Faulted or Segmented
S-1	Saucer	NW	E-W	264	12900	Not faulted
S-2	Saucer	NW	E-W	404	12330	Faulted
S-3	Anticline	NE	E_W	522	15440	Faulted
S-4	Elongated saucer	NW & NE	E-W	770	13320	Slightly faulted
S-5	Trapezoidal	NW	E-W	510	12440	Not faulted
S-6	Elongated	NNE	E-W	270	13060	Faulted
S-7	Saucer	SE	NW-SE	235	14610	Highly faulted
S-8	Adulatory saucer	NWN	NW-SE	165	14750	Segmented & faulted
S-9	Fish shape	NW	NW-SE	840	12850	Faulted
S-10	Elongated	S	E-W	690	13890	Faulted & segmented
S-11	Elongated dome	NS	N & S	480	18860	Faulted
S-12	Elongated	NW	E-W	460	13100	Faulted & segmented

Sill S-3 is almost parallel and overlying to the Sill S-2 (Fig. 3). Due to the lack of data, the eastern edge of the sill appears straight. The sill, in general, is concordant with the hosting strata.

TABLE III
SOME STATISTICS OF THE SILLS IN THE STUDY AREA, CALCULATED FROM THE PRODUCED MAPS AND SEISMIC SECTIONS

Sill name	Long axis (km)	Short axis (km)	Minimum 2WT Depth (sec)	Maximum 2WT Depth (sec)	Thickness 2WT (sec)	Area km^2
S-1	6.75	3.58	1.86	2.29	0.040	23.11
S-2	6.50	3.9	2.20	2.49	0.056	22.42
S-3	9.00	3.7	2.35	2.75	0.040	30.4
S-4	12.00	2.19	2.27	2.48	0.032	16.944
S-5	4.94	2.40	1.81	2.15	0.034	13.54
S-6	6.30	1.3	2.39	2.66	0.038	9.30
S-7	6.70	2.25	2.44	2.58	0.039	14.82
S-8	7.00	1.6	2.18	2.42	0.038	13.833
S-9	5.204	1.45	2.03	2.41	0.026	6.939
S-10	12.96	1.894	1.47	1.62	0.028	21.232
S-11	10.50	2.34	1.49	1.60	0.036	18.46
S-12	8.95	2.17	1.70	1.90	0.030	21.61

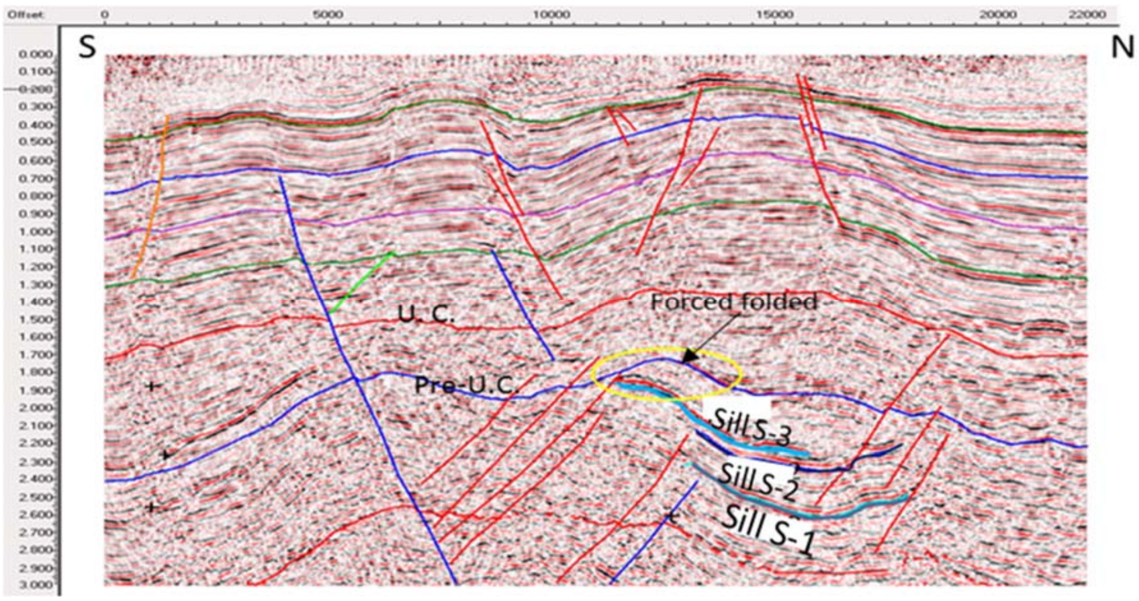

Fig. 7 Seismic line showing a group of faults affecting the continuity of sills S-1, S-2, S-3

Sill S-4 is in the middle of the eastern part of the study area and is also elongated east-west. The sill has a saucer shape with the eastern part dipping NW, and the western part dipping NE (Fig. 6).

Sill S-5 located in the eastern part of Enaga-5 was crosscut by a group of faults, particularly at the west. The plan view reveals the trapezoidal shape with the long base to the south (Figs. 4 and 8 (a)). When tracing the sill through the in-line seismic sections, it is found that the sill is dipping northward, mostly consistent with the host rock layers. It is closely linked at its western tip with the sill S-3, while at the eastward both sills are overlapping each other.

Sill S-6 composed of three segments, the western one dipping to the north, the middle one dipping north-northeast, while the eastern segment dipping to the south. The sill characterizes with an uneven edge elongated shape (Fig. 8 (b)).

Sill S-7, on the inline profiles, is concave up. Moving eastward through the profiles the dip of the sill turns northward. The western half of the sill is wider than the eastern one (Fig. 8 (c)).

Sill S-8 is located approximately at the middle of the study area, it has an undulated surface (Fig. 8 (d)). The shape turns to a northward dipping sheet as moving eastward. The surface of the sell dominated by several faults that affected its amplitude and continuity (Fig. 12 (b)).

Open Science Index, Geological and Environmental Engineering Vol:16, No:10, 2022 publications.waset.org/10012720.pdf

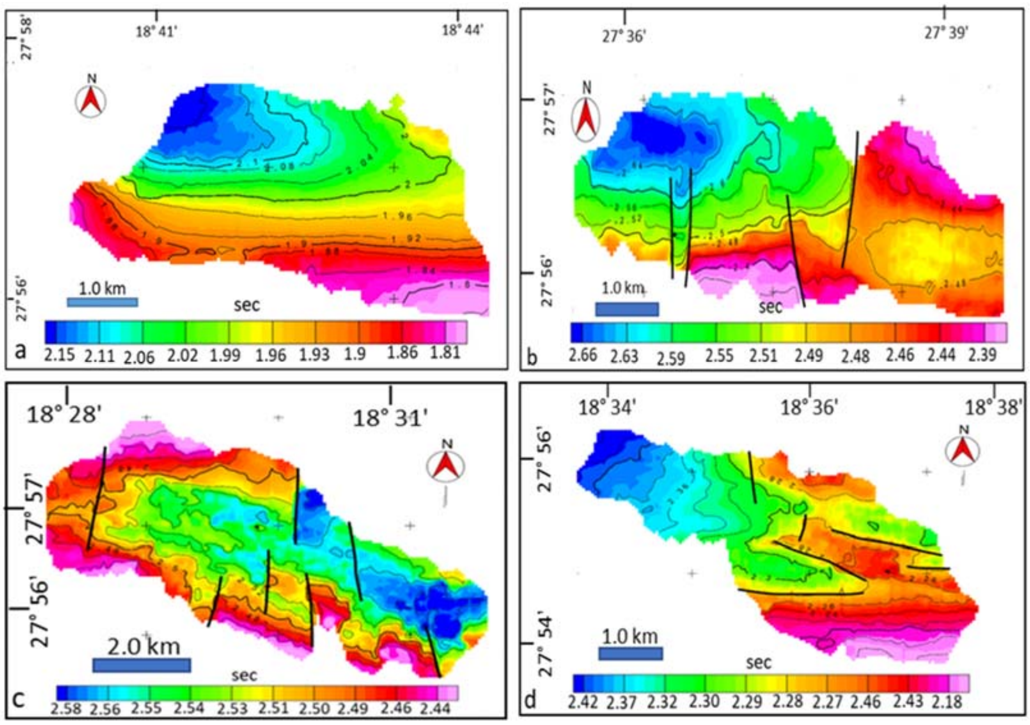

Fig. 8 Plan views of number of sills, (a) sill S-5 (b) sill S-6, (c) sill S-7, and (d) sill S-8

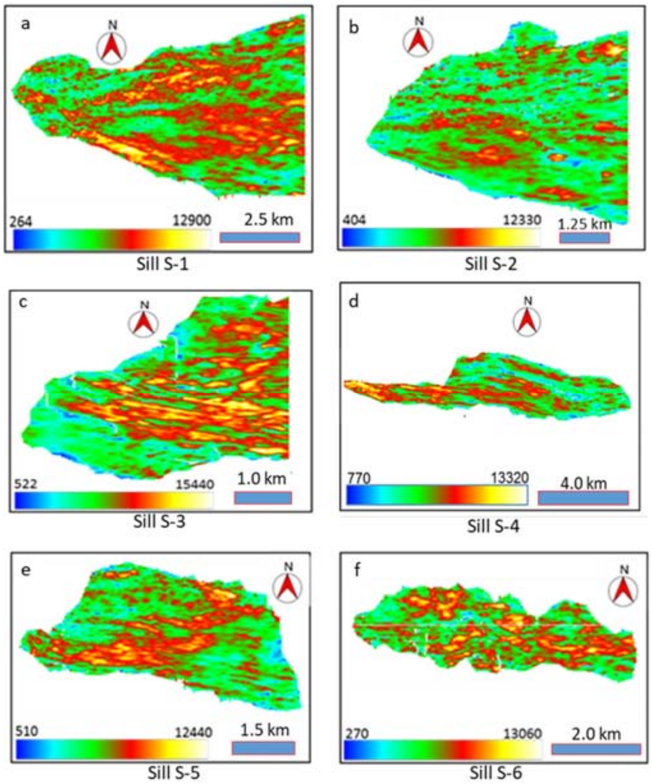

Fig. 9 The amplitude variation of the detected sills

Sill S-9 is dipping NW (Fig. 11 (a)), it is rising and then flattening towards the SE. N-S profiles reveal the curved dipping shape of the sill that. Sill S-10 located in the central part of the area of study, (Fig. 11 (b)), the westernmost part of the sill area is split into two segments. Sill S-11 located in the eastern part of the area, as moving westward the sill become narrower (Fig. 11 (c)). The sill along N-S profiles looks like a sinuous sheet harmonious with the hosting strata (Fig. 13). Sill S-12 was emplaced at the middle right part of the study area, its width decreasing westward (Fig. 11 (d)), several faults have a noticed impact on its amplitude and continuity. The sill as moving westward tends to be horizontal and the dipping turns to the south. At the far west, the sill is divided into two segments, one of which stays at about the same depth until it connects to another sill, while the other segment rising gradually as going westward.

V. Estimating the Emplacement Time and the Intra-Relationships between the Interpreted Sills

It is noticeable that the first three sills S-1, S-2, and S-3 are nearly emplaced parallel to each other, the syncline structure of their host layers controlled the shape of these sills (Figs. 3 and 7) The continuity of the sills that intruded into the pre-upper Cretaceous strata is largely affected by the faults that dominated the strata of this age, while the above layers have an anticlines shape (Fig. 13).

The northern side of sill S-5 and the south-western part of sill S-3 have linked each other (Figs. 3 and 13). Sill S-2 is incubating the sill S-3. S-1 and S-10 are the deepest and the uppermost sills in the group respectively, S-1 rooted nearly at the top of the basement, and S-10 is laying into the Upper Cretaceous sequence (Fig. 10). Tracing of sill S-2 and sill S-3 along the seismic profiles shows that they are approaching gradually each other, heading west until finally quite merging. N-S profiles reveal the sharply escalating sill S-4. Most of the interpreted sills are impacted and affected by the considerable number of faults that strike in different directions and extending vertically from the surface to the top of basement. This means that the sediment sequences are the oldest event in which the sills were emplaced then recently the younger faults took place. The present-day depths of Sills S-1, S-2 though S-9 are the pre-Upper Cretaceous, while sills (S-10, S-11, and S-12) intruded into the Cretaceous unit.

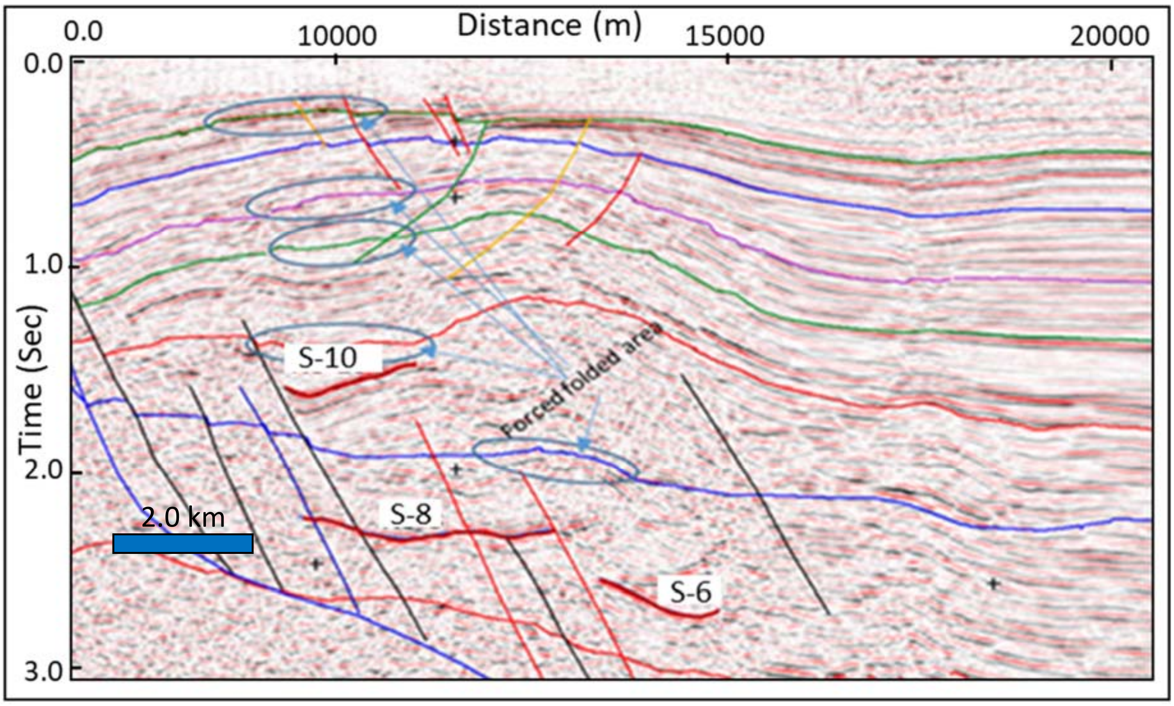

Fig. 10 3D Seismic profile illustrating the sills S-6, S-8 and S-10, note the slightly forced folded over adjacent tips of sills S-6 and S-8 and over the sill S-10

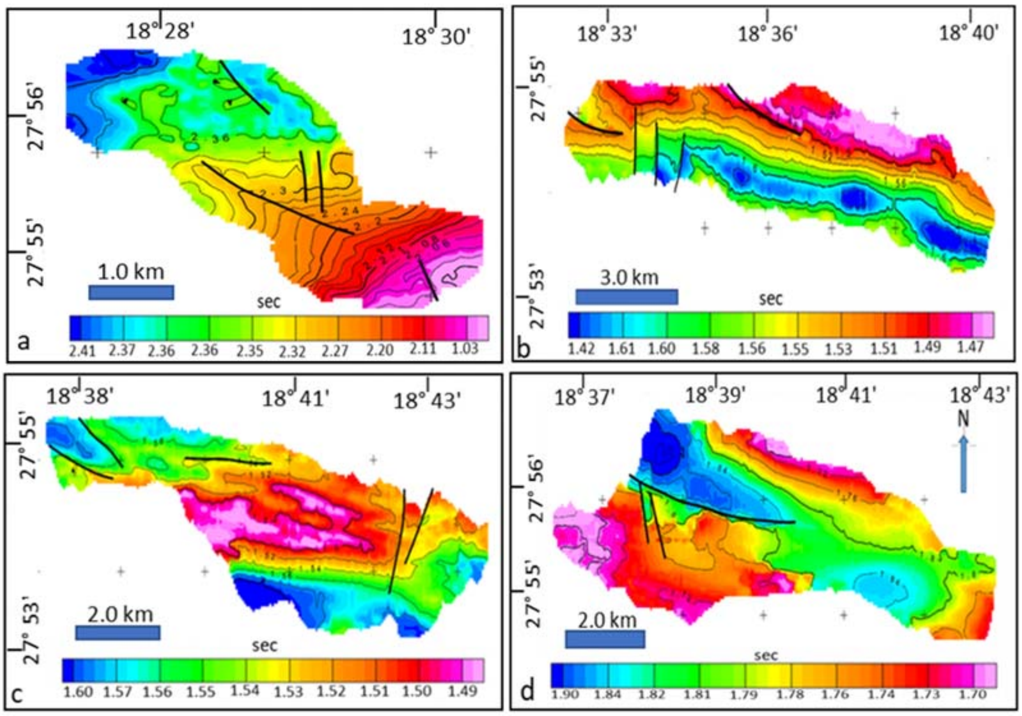

Fig. 11 Plan views of number of sills, (a) sill S-9 (b) sill S-10, (c) sill S-11, and (d) sill S-12

Open Science Index, Geological and Environmental Engineering Vol:16, No:10, 2022 publications.waset.org/10012720.pdf

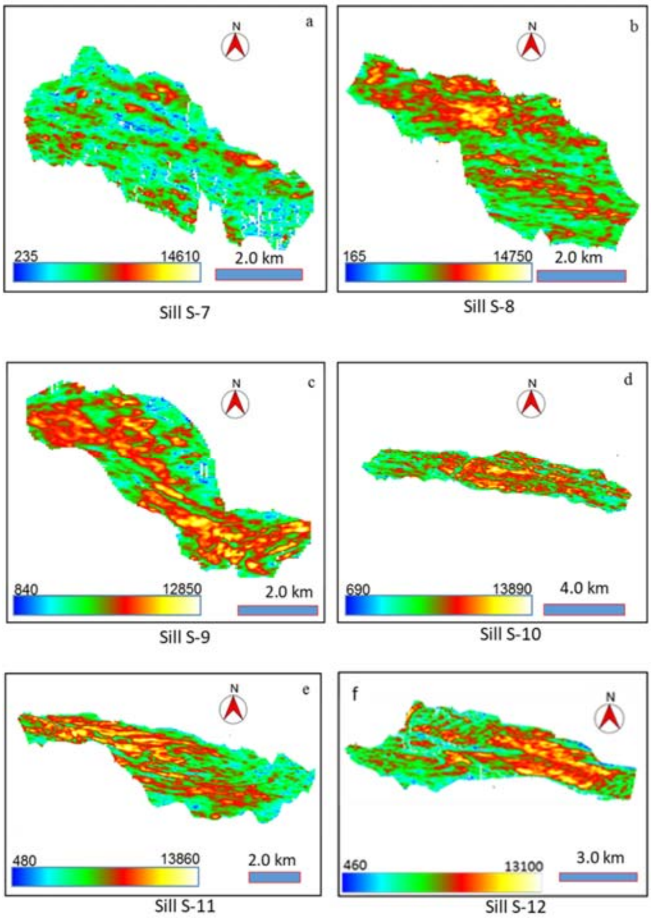

Fig. 12 The amplitude variation of the detected sills

The pre-Upper Cretaceous surface has experienced a slightly forced folding over the deepest three sills S-1, S-2 and S-3 (Fig. 10), this event exists also above the left and right tips of sill S-6 and S-8 respectively, while it is lacking and not noticed on the upper sequences of layers; this probably means that the mentioned sills were emplaced during the early-Upper Cretaceous time.

The Upper Cretaceous sequence is predominated by abundant faults, some of these faults caused the sill S-10 and sill S-11 to have a feeding relationship (Fig. 13). It is proposed that the sill S-10 emplaced after the deposition of the Eocene due to the clear impact of this sill on the above sequences including the Eocene (Fig. 13). From the previous observations, the question must be answered: whether the two different emplacement levels and the structural events that associated occurred in different periods (Cretaceous then Oligocene), or both occurred at the time of Oligocene. Based on the noticed events, the first proposal is more appropriate, and if that is the situation, then the deeper sills can be considered to have occurred during the volcanic activity associated to the Tibesti-Sirt Arch rift, which is believed to have occurred in the Cretaceous, probably because of the mantle hotspot [16], whereas the shallower sills probably belong to the eruptions of the Oligocene volcanic. The second scenario is also possible, given the assumption that the depth of the pre-Upper Cretaceous sills was quite enough to prevent the impact of these sills on the shallow layers above the Cretaceous, and all the emplacement sills were related to the Oligocene volcanic events.

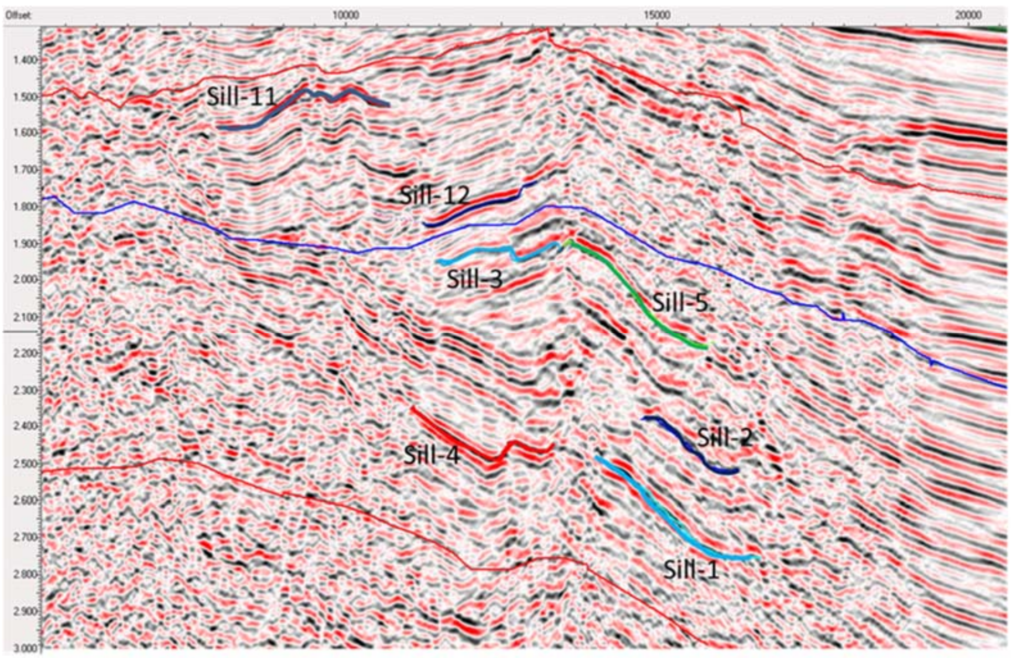

Fig. 13 The shape of a group of sills in the N-S 3D seismic profiles

Open Science Index, Geological and Environmental Engineering Vol:16, No:10, 2022 publications.waset.org/10012720.pdf

Open Science Index, Geological and Environmental Engineering Vol:16, No:10, 2022 publications.waset.org/10012720.pdf

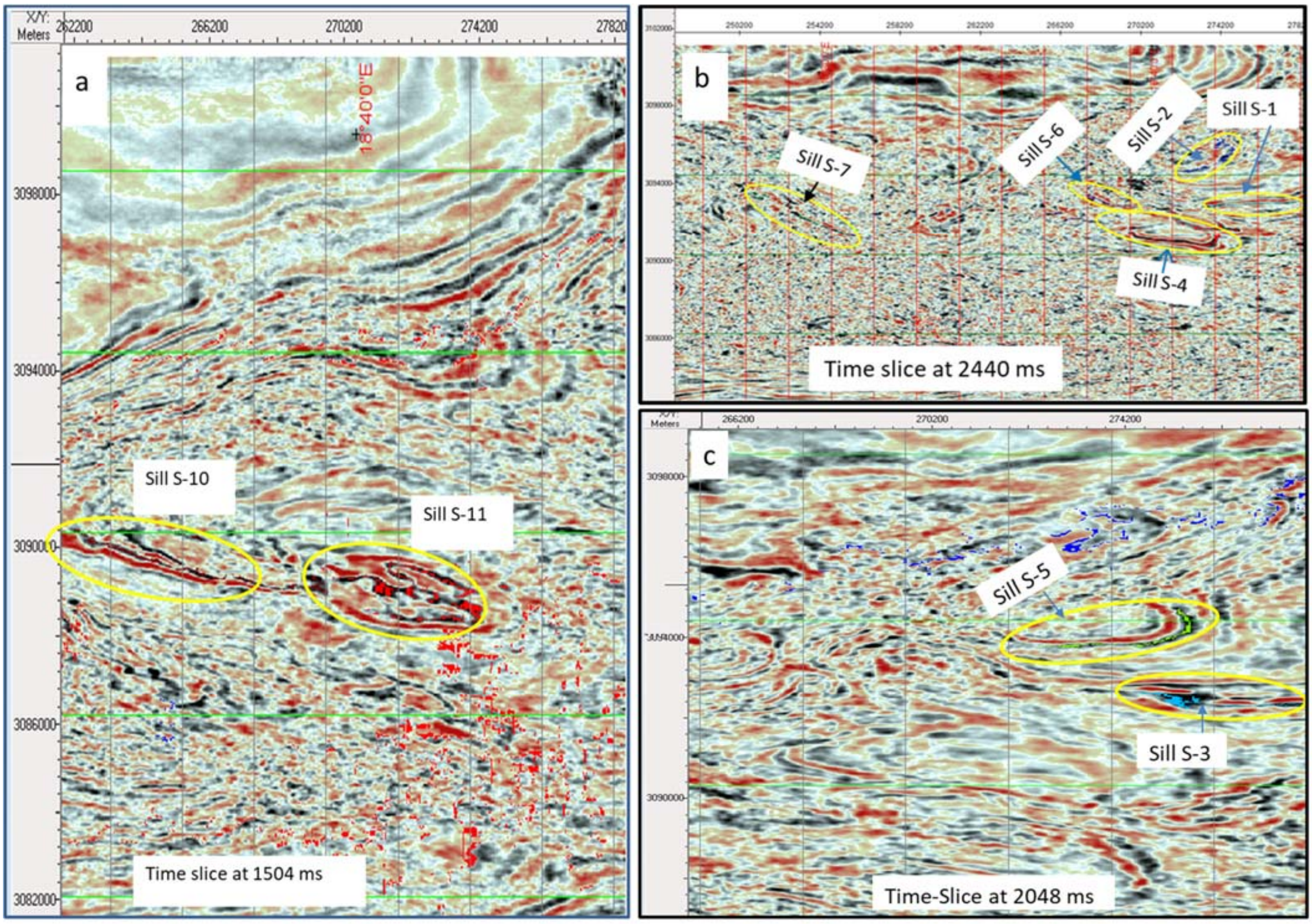

Fig. 14 The interpreted sills in the horizontal seismic sections

VI. Conclusion

- The study area is dominated by a significant number of sills, intruded into the Pre-Upper Cretaceous and early Upper Cretaceous depositions
- Most of the interpreted sills are intruded during the Upper Cretaceous time due to the Tibesti-Sirt Arch rift, and the others are probably emplaced after the Eocene (due to the Oligocene volcanic eruptions).
- The deepest sills have been affected by the tectonics events that the basin underwent during the Cretaceous time.
- The host rock situation controls the configuration of the sills and their shapes during the time of emplacement.
- Feeder relationship is noticed between some sills due to the existence of the faults.
- The existence of minor faults and fractures in the study area offered paths and ways for the propagation of the magma. Therefore, the deformation of the hosted rock due to the magma propagation has been reduced.
- Compared with the sills emplaced globally the interpreted sills in the study area are characterized by relatively small areas

References

[1] McKenzie, D., and Peate Bickle M.J. (1988) The volume and composition of melt generated by extension of the lithosphere, J. Petrol., vol. 29 (3), p. 625-679.

[2] McKenzie, D.P. (1985) The extraction of magma from the crust and mantle: Earth Planetary Science Letters, v. 74, p. 81-91.

[3] Pitcher, W. S. (1993) The Nature and Origin of Granite. Second edition, Chapman and Hall, London.

[4] Wilson, M., and Guiraud R. (1998) Late Permian to Recent magmatic activity on the African-Arabian margin of Tethys, in D. S. Macgregor, R. T. J. Moody, and D. D. Clark-Lowes, (eds.)

[5] Sandford, K.S. (1935) Geological observations on the north-west frontiers of the Anglo-Egyptian Sudan and the adjoining part of the southern Libyan desert. Quart. Journ. Geol. Soc. London, vol. 91, p. 323-381.

[6] Schurmann, H.M.E. (1974) The Pre-Cambrian in North Africa. Netherlands. Brill, Leyden.

[7] Cahen, L., Snelling, N.J., Delhal, J. and Vail, J.R. (1984) North-East Africa and Arabia. In: The geochronology and evolution of Africa. Clarendon Press, Oxford, chap. 14, p. 254-269.

[8] Morgan, M.A., Grocott, J. and Moody, R.T.J. (1998) The structural Baudet, D. (1988) Precambrian palynomorphs from northeast Libya. In: Subsurface palynostratigraphy of northeast Libya, (eds.) A. El-Arnauti, B. Owens and B. Thusu). Research Centre, Garyounis University, Benghazi, p. 17-26.

[9] Oun, K.M., Liegeois, J.P. and Daly, S. (2000). Evolution of the Pan-African Jabal al Hasawnah granites (abstract only). Second Symposium on the Sedimentary Basins of Libya, Geology of Northwest Libya. Book of abstracts, p. 71.

[10] Baudet, D. (1988) Precambrian palynomorphs from northeast Libya. In: Subsurface palynostratigraphy of northeast Libya, (eds.) A. El-Arnauti, B. Owens and B. Thusu). Research Centre, Garyounis University, Benghazi, p. 17-26.

[11] Banerjee, S. (1980) Stratigraphic Lexicon of Libya. Bulletin No. 13. Industrial Research Centre, Tripoli, p300.

[12] Van Houten, F.B. (1983) Sirt Basin, north central Libya; Cretaceous rifting above a fixed mantle hotspot, Geology, vol. 11, p. 115-118.
[13] Hallett, D. (2002) Petroleum Geology of Libya, Amsterdam: Elsevier.
[14] Gumati, Y.D., (1985) Crustal extension, subsidence, and thermal history of the Sirte Basin, Libya. ESRI Occasional publication No.3. Columbia, S. Carolina, 207p
[15] Polteau, S., Mazzini, A., Galland, O., and Planke S. (2007a), Saucer-shaped intrusions: Occurrences, emplacement and implications, Physics of Geological Processes, University of Oslo, Oslo, Norway.
[16] Dercourt, J., Zonenhain, L.P., Ricou, L.E. et al. (1986) Geological evolution of the Tethys belt from the Atlantic to the Pamirs since the Lias. Tectonophysics, vol. 123: p. 241-315.

#

Open Science Index, Geological and Environmental Engineering Vol:16, No:10, 2022 publications.waset.org/10012720.pdf